



HAL
open science

Ag and Pb isotope systematics in galena ores from southern Sardinia and southern France flag potential silver sources in antiquity

Francis Albarede, Maria Boni, Janne Blichert-Toft, Markos Vaxevanopoulos, Katrin Westner, Jean Milot, Marine Pinto, Philippe Télouk

► To cite this version:

Francis Albarede, Maria Boni, Janne Blichert-Toft, Markos Vaxevanopoulos, Katrin Westner, et al.. Ag and Pb isotope systematics in galena ores from southern Sardinia and southern France flag potential silver sources in antiquity. *Archaeological and Anthropological Sciences*, 2024, 16 (8), pp.118. 10.1007/s12520-024-02025-1 . hal-04651711

HAL Id: hal-04651711

<https://hal.science/hal-04651711>

Submitted on 17 Jul 2024

HAL is a multi-disciplinary open access archive for the deposit and dissemination of scientific research documents, whether they are published or not. The documents may come from teaching and research institutions in France or abroad, or from public or private research centers.

L'archive ouverte pluridisciplinaire **HAL**, est destinée au dépôt et à la diffusion de documents scientifiques de niveau recherche, publiés ou non, émanant des établissements d'enseignement et de recherche français ou étrangers, des laboratoires publics ou privés.

Ag and Pb isotope systematics in galena ores from southern Sardinia and southern France flag potential silver sources in antiquity

Francis Albarede,
Ecole Normale Supérieure de Lyon and CNRS, 69007 Lyon, France, email : albarede@ens-lyon.fr

Maria Boni,
Dipartimento Scienze della Terra, dell'Ambiente e delle Risorse (DiSTAR), Università di Napoli "Federico II", Italy

Janne Blichert-Toft, Markos Vaxevanopoulos, Katrin Westner, Jean Milot, Marine Pinto, and Philippe Télouk
Ecole Normale Supérieure de Lyon and CNRS

Abstract.

While lead isotopes serve to determine potential ore provenance, silver isotopes help evaluate if a specific ore flagged by Pb isotopes has actually been exploited as a silver source of bullion in antiquity. The combination of Ag and Pb isotopes thus constitutes a powerful tool to address provenance and identify potential ore sources. It has recently been observed that the vast majority of silver isotopic abundances in hundreds of silver coins from different historical periods (pre-Roman and Roman, Middle Ages, early modern times) and different localities (Persia, Greece, Rome, Western Europe, England, Spanish Americas) falls in a remarkably narrow interval (± 0.1 permil, or ± 1 on the epsilon scale used by geochemists to enhance the visibility of small differences, group 1). Five Greek coins and some pieces from Levantine *hacksilber* hoards dated to the Late Bronze and Early Iron Ages have isotopic abundances somewhat below the range of group 1 (-0.2 to -0.1 permil, or -2 to -1 on the epsilon scale, group 2).

The coverage of Ag isotopes in ores from the western Mediterranean, with the exception of Iberia, is inexistant. Here the above-mentioned approach is illustrated with new Pb and Ag isotopic analyses of samples from southern Sardinia and southern France. The majority of Ag isotope compositions of galena samples from Sardinia belong to group 2 and none to group 1. While scholarly works imply that Sardinia may have provided silver to the Levant during the Iron Age, the exact location of the Sardinian ores that contributed to classical and archaic Greek coins is still unknown. Galena samples from southern France (the Pyrenees, Montagne Noire, Cévennes) are characterized by Ag isotope compositions from both groups 1 and 2, indicating that silver-bearing ore deposits in Gaul could be considered a potential source for silver bullion, both before and during the Roman era.

Introduction

Lead isotope databases such as OXALID (Stos-Gale and Gale, 2009), IBERLID (de Madinabeitia et al., 2021), TerraLID (its prototypes were introduced as GlobalID) (Klein et al., 2022), and the Lyon database (Milot et al., 2021a, Milot et al., 2021b, Vaxevanopoulos et al., 2022, Westner et al., 2023) hold almost 7000 Pb isotopic data entries on galena and other less common potential ores spread over the entire Western Europe, the circum-Mediterranean regions, and the Middle East. Although radioactive decay of uranium and thorium makes the variability of Pb isotope compositions very large, the sheer number of samples present a real technical challenge for assessing the provenance of silver artifacts. Mixed bullion adds complexity to these attempts; however, the problem of mixing was recently addressed with some arguable success by our group (Albarede et al., 2024b).

The challenge presented by silver isotopes is very different. In contrast to the abundances of Pb isotopes, which reflect the tectonic age of ore formation and the U/Pb and Th/Pb of its source(s) (Albarède et al., 2012), isotope fractionation of the two isotopes ^{107}Ag and ^{109}Ag in natural fluids and minerals is controlled by the energetics of Ag bonds in molecular species and the temperature of hydrothermal solutions (Fujii and Albarede, 2018, Wang et al., 2022). Silver isotope fractionation becomes vanishingly small for solutions hotter than 400°C and does not occur during the metallurgical process until the metal is almost completely evaporated (Berger et al., 2021). Silver isotopes should not, in general, be regarded as true provenance markers and are not expected to co-vary with Pb isotopes. The range of Ag isotope abundances measured in silver coinage of different ages spanning from the end of the Iron Age to modern times, in an ample field of geographical origins across several continents (Europe, Asia, Africa, Americas) is only a few parts per 10,000 (Fujii and Albarede, 2018). In contrast, the range of silver isotope compositions displayed by the most common silver ores (galena (PbS), several types of Ag-sulfosalts, acanthite (Ag_2S), and native silver from hydrothermal deposits (Arribas et al., 2020)) is an order of magnitude broader (Fig. 1). Such a contrast indicates that one very particular type of ore dominates the sources of the bullion used for silver coinage. Silver is not extracted from a multitude of different ores, but from galena and its low-temperature alteration products, such as sulfides and sulfates. A positive consequence of this observation is that, while Pb isotope compositions of galena and other silver-rich ores help identify potential 'candidate' bullion sources, silver isotopes help weed out a large fraction of the same candidates (Milot et al., 2021b, Milot et al., 2022, Vaxevanopoulos et al., 2022, Westner et al., 2023). When combined with archaeological evidence and ancient literary testimony, the pruning of potential silver sources and the identification of so-far unnoticed alternative ore districts using silver isotopes therefore may be of great historical value. Silver and lead isotopes are not provenance tracers in the same way, but they complement each other and, when used together, constitute a powerful provenance tool.

In order to document the complementarity of Pb and Ag isotopes, let us summarize the current state of Ag isotopes research in Archaeology. Over 95% of the silver coins and artifacts from ancient Greece, the Roman Republic and Early Empire, Medieval Europe, and Spanish

Americas analyzed for silver isotopes have $\epsilon^{109}\text{Ag}$ values¹ falling within the range of -1 to $+1$ (Albarède et al., 2016, Desaulty et al., 2011, Desaulty and Albarede, 2013, Eshel et al., 2022, Milot et al., 2021b, Milot et al., 2022, Vaxevanopoulos et al., 2022). These values will hereinafter be referred to as the ‘main range’ or group 1. Some rare Greek coins (Vaxevanopoulos et al., 2022) of smaller denominations, several Roman-period coins from the Balkans (Westner et al., submitted), and pieces of *hacksilber* (chopped bits of silver) from hoards in the Levant (Eshel et al., 2022) are isotopically lighter, hence falling outside the main range with $\epsilon^{109}\text{Ag}$ values between -1.9 and -1.0 . These are hereinafter referred to as group 2.

For Ag to be used as a provenance tool to its full extent, the geographical coverage of Ag isotopes in potential ores around the ancient Mediterranean world must be expanded. The purpose of the present study is to do exactly that: expand the Lyon Pb and Ag isotope database to Sardinia and, by geological extension, also to southern France, because of their geological similarity and potential historical interests. Ancient Sardinia and Gaul are not widely perceived as major sources of silver, at least not on par with mining districts in the southern Aegean, Thrace, Macedonia, and Iberia. The galena and sulfosalt ores in the small districts of Northern Sardinia, though having been exploited in the past, are not rich enough in silver to have provided abundant bullion. Argentiera is the only silver-rich lead deposit (Orlandi and Gelosa, 2007) characterized by Pb-isotopic values that differ from those of the Iglesiente ores (Eshel et al., 2019).

The scarcity of Bronze Age silver artifacts found in Sardinia has been interpreted as indicating little mining activity of argentiferous ores in Sardinian chiefdoms during this period (Terpstra, 2021, Valera et al., 2005b). Nevertheless, recent Pb isotope studies reveal that Nuragic populations traded silver from the geologically older southern Sardinia with the Levant in the early Iron Age (Eshel et al., 2019, Eshel et al., 2021, Gentelli et al., 2021) (see also Pearce’s (2017) review). At even later times, lead isotope data found in Archaic coinage of Athens, Corinth, and Aegina, are consistent with a small but distinctive contribution of South Sardinian-like silver (Albarede et al., 2024a) interpreted as some sort of ‘cash float’ of trade between Greece and southern Italy. By contrast, intensive exploitation of the deposits in the Iglesiente mining district by Carthage and the Romans after the First Punic War is attested to in the literature (Ingo et al., 1996, Valera et al., 2005a).

Since Sardinia once belonged to the Hercynian margin of southern France and Catalonia until the Late Oligocene (~ 30 Ma) (Cherchi and Montadert, 1982, Jolivet and Faccenna, 2000, Puddu et al., 2021, Rehault et al., 1984, Romagny et al., 2020, Schettino and Turco, 2011) and, together with Corsica, was embedded in an eastern extension of the Pyrenees (Casas, 2010), we analyzed samples from southern France as well as samples from Sardinia. Extending our reconnaissance area in this way is further justified by lead isotope provenance studies pointing to ore deposits in southern France as potential bullion sources for *hacksilber* (Gentelli et al., 2021) and Archaic coinage (Stos-Gale and Davis, 2020).

¹ $\epsilon^{109}\text{Ag}$ of a given sample is defined as the relative deviation of its $^{109}\text{Ag}/^{107}\text{Ag}$ ratio from that of the reference material NIST 978. This deviation is usually reported in parts per 10,000 due to the small isotopic differences displayed by Ag. Because this is the well-known standard usage, the cumbersome factor of $\times 10^{-4}$ is left unwritten. Note that, for ease of comprehension in the abstract, the range of Ag isotopic compositions is given there in the more familiar unit of permil, which is parts per 1000 (a factor of $\times 10^{-3}$).

To summarize, the present work presents new high-precision Pb and Ag isotopic data for a whole region of the western Mediterranean which up until now was devoid of Ag isotope data. This new data set allows us to test whether Sardinia and southern Gaul are acceptable sources of bullion used to mint ancient silver coinage. Although access to abandoned mines and ore deposits in this region is limited and in most cases impossible, we nevertheless managed to obtain a total of 26 galena ores from southern Sardinia and southern France (13 samples from each region) from old mine heaps and collections. We then combined the newly measured values with literature data and reviewed the occurrences of potential circum-Mediterranean sources that may satisfy the 'Ag isotope condition' (*a.k.a* the 'main range' or group 1, but also group 2) mentioned above. Identifying plausible sources of bullion around the western Mediterranean using Ag isotopes (in combination with Pb isotopes as explained above) is the prime objective of the present work.

Geological setting

The geology of southwestern Sardinia is largely dominated by sedimentary Cambro-Ordovician rocks (Fig. 2). The geological units in the Iglesias-Sulcis mining district consist of low-grade metamorphic rocks, belonging to the so-called "External zones" of the Variscan orogen (Franceschelli et al., 2005). The Lower Cambrian succession is subdivided into the basal Nebida Group and the overlying Gonnese Group, which consists of carbonate rocks hosting Zn-Pb mineralization considered as sedimentary-exhalative (Sedex) and large, carbonate hosted, massive sulfide Zn/Pb (Irish-type) ore deposits (Bechstadt and Boni, 1994, Boni et al., 1996, Santoro et al., 2023). The Cambrian sediments were deformed by a first tectonic phase in the upper Ordovician (the Sardic phase). At the end of the major Variscan orogeny, the Lower Paleozoic basement was intruded by post-collisional granites, which caused the formation of skarn-type deposits. Variscan tectonics and magmatism were followed by a long continental period, associated with erosion and deep karstification of the Cambrian carbonates, which periodically underwent hydrothermal dolomitization episodes. From the Permian onwards, southern Sardinia experienced several hydrothermal phases comparable to those having occurred in other European terranes. The associated ores consist of low-temperature veins and paleokarst breccia fillings in the Cambrian carbonates, which contain mainly Ag-rich galena and barite mineralizations (Santoro et al., 2023).

The Montagne Noire is the southern extension of the French Massif Central (Fig. 3). It consists of three main structural domains: (1) a metamorphic axial zone made up of complex domes of gneiss and migmatites surrounded by micaschists; (2) a northern flank composed of imbricated tectonic nappes of Cambrian to Silurian rocks; and (3) a southern flank made up of large nappes involving Cambrian to Carboniferous strata (Alvaro et al., 2008). In the Montagne Noire, carbonate rocks were deposited during part of the Cambrian, as in the Iberian Peninsula and Sardinia. At the southern edge of the Massif Central, in a region known as the Cevennes, several nappes are correlated with those of the northern Montagne Noire. In Les Malines mining district the two southernmost units are exposed, represented by Les Malines 'autochthonous' and overlying Saint Bresson units. The Cambrian stratigraphic record of the above units is an analogy to the northern Montagne Noire, in the broad terms of paleogeographic and paleotectonic evolution. The stratigraphic position of the northern Montagne Noire Sedex-type mineralization corresponds roughly to that of the mineralization

at Sanguinède and Montdardier in the Cévennes (Orgeval et al., 2000). An exception is represented by the classic Les Malines mine ores, which are of Triassic age (Orgeval et al., 2000). In contrast to the Sedex-type occurrences of the northern Montagne Noire, the southern Montagne Noire deposits, set in a shallow carbonate platform, are considered as Mississippi Valley-type (Lescuyer and Giot, 1987, Marignac and Cuney, 1999) and can be compared with part of the Pb ores of the Iglesias in Sardinia. In between the Cévennes and the Montagne Noire there is a small area consisting of Late Proterozoic and Cambrian terranes intruded by the Mendic granite of terminal Ediacaran age (Leveque, 1990).

Several recent reviews and monographs on the Variscan basement of the Pyrenees have been published by (Casas et al., 2019, Denèle et al., 2014, Guitard et al., 1995, Laumonier et al., 2008). The axial zone of the Pyrenees, which hosts part of the samples analyzed in this study, has been involved in two pre-Alpine events: the Cadomian event (= pan-African) across the Proterozoic-Cambrian boundary, and the Carboniferous Variscan event (= Hercynian). Discontinuities contemporaneous with the Ordovician Sardinic phase are ubiquitous in this area.

Sampling and Analytical techniques

Ore sampling has become a modern challenge. For safety and liability reasons, most major abandoned mine shafts in several European countries have been blasted, flooded, and sealed to prevent the intrusion of unprotected collectors. An even more pervasive limitation is the shrinking space dedicated to public rock collections stored and curated by universities and other academic institutions. The field of ore geology and its perception by the public has considerably changed over the last few decades. As large numbers of researchers with skills in Ore Geology have retired, the space that was dedicated to their ore and rock collections has been reassigned to newly developing fields, and the collections themselves have been scattered, discarded, or moved to premises inappropriate for conservation. We therefore were limited to rare, unfortunately often poorly documented, but always properly curated samples that had been preserved in collections accessible at the University of Naples and the Museum of the École des Mines de Paris. Additionally, several samples were personally collected by one of us (M.B.) in SW Sardinia.

Most of the samples analyzed in the present study consist of galena, with the exception of the bournonite (PbCuSbS_3) sample 63600 from the Cambrian-late Proterozoic terranes of Brusque and the cerussite sample S-38 from Les Malines (Cévennes). The names and origins of all the samples are listed in Table 1.

In southern France, we sampled three distinct units of Variscan crust, which have a very similar geological history: the Montagne Noire, the Cévennes, and the axial zone of the Pyrenees. In the Peyrebrune district (samples 59051, 59040, and Tarn), west of the Montagne Noire, predominantly Zn-(±Pb)-F veins occur emplaced in early Paleozoic schists (Munoz, 1997), which were already exploited by the Gauls. To the north-east of the Montagne Noire (Brusque, sample 63600), strata-bound Pb-Zn ores are found in Cambrian carbonates (Guérangé-Lozes et al., 1982). In the Cévennes, the samples from Les Malines and Durfort (samples 63025, S-38, and Durfort) belong to multiple ores deposited during successive phases in Paleozoic and Triassic carbonates (Le Guen et al., 1991). The axial zone of the Pyrenees contains sedimentary-exhalative Pb-Zn deposits formed during the Paleozoic (Aulus-Argentière,

sample 65644 and 65649; Aulus-Lauqueille, sample 65726; Seix, sample 65647; Abères, sample 65826). Vein-type mineralizations within Late-Silurian and Devonian calcschist and limestone apparently produced significant amounts of silver (Munoz et al., 2016), although the details of how much bullion was extracted from these remote and high-altitude mines at any given time remain essentially unknown. Fragments of amphoras found in gullies indicate that these mines were known since at least Roman times. An inventory of Pb-Ag ores is available for the zone of interest, known as Couserans (the Ariège department), in Dubois (1997) and an updated discussion on Pyrenean ore mineralogy can be found in Cugerone (2018).

The techniques used to measure trace element concentrations and purify silver and lead for high-precision isotope analysis by MC-ICP-MS are fully described in (Milot et al., 2021a, Milot et al., 2021b, Vaxevanopoulos et al., 2022, Westner et al., 2023). For two samples, 'Tarn' and 'Durfort', there was not enough Ag for high-precision isotopic analysis. We suspect that, for these two samples, the low-yield Ag separation resulted from unusually large abundances of organic material in the ores interfering with the column chromatography.

Results

Binary plots of Pb isotopic ratios are often misleading because they account poorly for the 3-dimensional character of the data (Albarède et al., 2020): inclusion of a given data point in the projections of a 3-dimensional field in two 2-dimensional plots is not sufficient to demonstrate that the data point in question is part of the original 3-dimensional field. Nevertheless, to comply with the usual practice of Archaeometry, Pb isotopic ratios have been plotted in Fig. 4 in the conventional manner. To avoid overcrowding the figures, only ore samples for which both Ag and Pb isotope compositions are currently available are plotted, whether this be the conventional binary Pb isotope plots or the maps of Fig. 5-7, the latter of which emphasize regional clusters (Milot et al., 2022, Vaxevanopoulos et al., 2022, Westner et al., 2023). These maps therefore include both the new samples and those from the literature. Note also that on the maps overlapping points have been made visible by a small random 'jittering' around the true location. The precise locations of the samples are given in the original publications reporting the Pb isotope compositions.

The Pb isotope compositions of the galena samples analyzed here are consistent with geological and archeological literature data. This is the case for both Sardinia (Boni and Koepfel, 1985, Boni et al., 1996, Orgeval et al., 2000), the Pyrénées (Marcoux and Moelo, 1991, Marcoux, 1987, Munoz et al., 2016), and the southern and southeastern part of the Massif Central of France (Cévennes) (Baron et al., 2006, Brevart et al., 1982, Charef, 1986, Le Guen et al., 1991, Le Guen et al., 1992, Ploquin et al., 2010).

In general, the Pb isotope data are well regionalized (Fig. 5-7):

- $^{206}\text{Pb}/^{204}\text{Pb}$ and Pb model ages T_m show a sharp contrast between four groups: (i) Sardinia; (ii) Sierra Morena and Central Europe; (iii) northeastern Spain and southern France; and (iv) the coastal Betics, Serbia, North Macedonia, and Greece.
- As expected, $^{207}\text{Pb}/^{204}\text{Pb}$ and μ values show some communality between southern Sardinia and southern France. $^{208}\text{Pb}/^{204}\text{Pb}$ and κ values also show similarities.

- Low values of $^{208}\text{Pb}/^{204}\text{Pb}$ and high values of $^{208}\text{Pb}/^{206}\text{Pb}$ from southern Sardinia (Iglesiente) and Central Europe contrast with samples from the coastal Betics in southern Spain, Serbia, North Macedonia, and Greece. The Sierra Morena in south-central Spain and southern France are intermediate between the two groups.

Overall, Late Proterozoic and Early Paleozoic model ages are found in southern Sardinia and occasionally in the Sierra Morena and southern France (Fig. 7). Paleozoic ages are more common in south-central Spain, northern Spain, southern France, and central Europe, while Late Mesozoic and Cenozoic ages prevail in the coastal Betics, the Balkans, and Greece.

The ore samples analyzed for silver isotopes (Fig. 8) have been subdivided into three groups corresponding to the thresholds previously observed in silver coinage. The main range coinage group (group 1, color-coded in red) has $\epsilon_{109\text{Ag}}$ values ranging from -1 to +1 parts per 10,000 with respect to the NIST 978A reference material, and is consistent with 95% of the values observed in Bronze to Iron Age *hacksilber* hoards from the Levant, in coins from ancient Greece and Rome, in medieval European coins, and in coinage from Spanish Americas (16-18th C). A second, isotopically light group (group 2, color-coded in orange) is defined by its $\epsilon_{109\text{Ag}}$ values extending from -1 to -2 parts per 10,000, values that are found in some *hacksilber* hoards (Eshel et al., 2022) from the Levant and in a small number of archaic Greek coins (Vaxevanopoulos et al., 2022). The $\epsilon_{109\text{Ag}}$ values of the third group (group 3, color-coded in white), also referred to as 'external', fall outside the -2 to +1 interval and do not correspond to any silver coinage or artifacts known so far. No samples from Sardinia fall in the main group, while five of them fall in the isotopically light group, and the rest fall in the external group (Table 1).

Ores from regions covered by the broad denominations of Balkans, Macedonia, Thrace, and Greece make up most of the likely sources of silver for the main coinage group 1. Some ore deposits from the Sierra Morena, the eastern Central Pyrenees, the southern Massif Central (notably the mine of Peyrebrune), and central Europe also represent acceptable bullion sources for this group. Group 2 is represented by Sardinia, the coastal Betics, and ore deposits scattered over the Balkans, Thrace, Iberia, and southern France. In the context of currently available data of ancient artifacts, the external group 3 does not carry any particular meaning.

Discussion

As expected from the very different physical processes controlling Ag and Pb isotope variation, the correlation between $\epsilon_{109\text{Ag}}$ and the different Pb isotope ratios is weak and statistically non-significant at the 95% confidence level (correlation coefficient $r \sim \pm 0.4$). The existence of two regions with contrasting Pb isotope compositions (the Aegean vs the western Mediterranean, Figs. 5-7) nevertheless explains to some extent that r is not truly zero.

For Sardinia, the probability that the present samples belong to the main group 1 and therefore were actually used for coinage is statistically low. In contrast, values from the isotopically light group are clearly identified. The small number of samples, of course, places some limits on a broad generalization. Archaeological evidence nevertheless suggests that Sardinian metallurgy took off in the last quarter of the fifth millennium BCE or later (De Caro

et al., 2013, Pearce, 2017). Evidence for mining of argentiferous galena has been recorded from the Iglesias province, notably at the Monteponi and Montevecchio mines (Ingo et al., 1996, Valera et al., 2005a, Valera et al., 2005b). Eshel et al. (2019, 2022) observed that the Pb isotope ratios of ores from San Giovanni are consistent with the silver artifacts they analyzed. The chronology of the mining works is still incomplete. Craddock (1995) and Pearce (2017) suggested that, in early prehistoric times, silver may have been preferentially extracted from supergene acanthite (Ag_2S), cerargyrite (a.k.a., chlorargyrite AgCl), and argentiferous cerussite, which have since been mined away, rather than from hypogene galena and associated sulfosalts. Although, to some extent, these results may be a consequence of limited ore sampling, it seems unlikely that these rare minerals ever represented a major source of silver in Sardinia with respect to Ag-hosting galena. In addition, supergene Ag minerals display large $^{109}\text{Ag}/^{107}\text{Ag}$ fractionation with respect to hypogene galena (Arribas et al., 2020). A provisional conclusion hence is that at least part of the silver mined in Sardinia belongs to the isotopically light group ($-2 \leq \epsilon_{109\text{Ag}} \leq -1$) and should be recognized as such in silver artifacts and coins. However, further Ag isotope studies are warranted on Ag-rich ores (>1000 ppm) before the significance of Sardinia on the silver circuits will be firmly established.

The situation for silver mining is different during the Iron Age. Isotopically light silver similar to that characterizing group 2 has been found in *hacksilber* hoards from the Levant by Eshel et al. (2022). Evidence from the combined Pb and Ag isotope signatures is more difficult to interpret. Artifacts with a Sardinian Pb isotope signature do not have the Ag isotope characteristics of the present Sardinian ores. Using new software, which relies on Pb isotopes and takes mass-dependent fractionation into account to locate the provenance of samples (Albarede et al., 2024a), we confirm Eshel et al.'s (2022) general findings for some *hacksilber* hoards that the lead isotope compositions of the Tel Dor, 'Akko, and Meggido hoards (all from Early Iron Age I), and possibly those of Tel Keisan (Late Iron Age) (Eshel et al., 2018), point to a possible Pb source from Sardinia. The Sardinian Pb isotope imprint on Iron Age artifacts may therefore be occasionally strong. The $\epsilon_{109\text{Ag}}$ values reported by Eshel et al. (2022) for these hoards are, however, typical of the main group 1. The samples reported on by these authors from the Shiloh hoard do belong to the isotopically light Ag group, but their high $^{206}\text{Pb}/^{204}\text{Pb}$ values are not compatible with a Sardinian source. The search therefore must continue in order to identify silver ores from Sardinia that belong to the main group 1. Additional silver isotope data on potential silver ores are definitely a high priority for future research.

Likewise, the $\epsilon_{109\text{Ag}}$ values of five isolated coins from Cyzicus (Mysia), Corinth, Abdera (Thrace), Chersonesus (Thrace), and Caria vary between -1.04 and -1.92 (Vaxevanopoulos et al., 2022), while their Pb isotope compositions and tightly grouped Pb model ages (24-52 Ma) suggest Aegean sources. Some silver sources exist in Troad, Mysia, and Caria (Yigit, 2009, 2012), but only few Pb isotope data are available (Wagner et al., 1985). In either case, the dilemma is between isotopically light silver not being a reliable provenance tool and lead used for cupellation potentially coming from a source very different from the mine where the silver originated. If, as argued above, galena should be abundant wherever silver is exploited, the former conclusion takes precedence. Of course, other factors, such as the market price for lead, may enter the equation, as foreign lead transported by merchant ships may be more competitive than locally extracted metal. Lead ingots found in shipwrecks and particularly abundant in Roman times (Domergue and Rico, 2003, Tisseyre et al., 2008, Trincherini et al., 2001, Trincherini et al., 2009) attest to intense long-distance trade of this metal. Whether lead

of distant origins prevailed on Pb markets remains a topic for further investigations, at least for the East Mediterranean world.

Gentelli et al. (2021) suggested that some Iron Age *hacksilver* hoards from the Levant (Beth Shean, Tel Keisan, and Tel Dor) comprise pieces for which a southern Gaul origin is plausible, which the new provenancing software developed by Albarede et al. (2024a) confirms. The present work identified ores with $\epsilon_{109\text{Ag}}$ values similar to the main coinage group 1 in southern Gaul, east-central Pyrenees, southern Massif Central, and the Cévennes. An isolated value from Bourg d'Oisans in the French Alps (CRPG 1046, (Milot et al., 2021b)) is also part of this group. This is consistent with archeological finds of Ag mining activity from the Roman period in southern Gaul (Abraham, 2000, Baron et al., 2006, Bonsangue, 2011, Domergue and Leroy, 2000, Feugère and Py, 2007, Ploquin et al., 2010). Dubois (1997) argues that argentiferous galena was exploited from the Albères (maritime east Pyrénées) and Esplas-de-Séroux lodes (east-central Pyrenees) since Roman or even pre-Roman times, and mentions amphora fragments in gullies from the Couserans. Writing at the turn of the first millennium before the Roman conquest, the Greek historian and geographer Strabo mentions (3.2.8; 4.1.12; 4.2.2) silver mining in the lands of the *Ruteni* (southern Massif Central) and the *Gabales* (northern Cévennes) (see Hirt's (2020) review). In their review of Iron Age and Roman metallurgy, Domergue et al. (2006), possibly influenced by Diodorus Siculus (*Libr. Hist.* 5.27)², argue from observations of ancient mining works that Gaul was, overall, not a major silver-producing region, i.e., not on par with the Aegean and Iberia, neither under the Gauls nor under the Romans. However, both in the field and in ancient literature, statistics are inadequate. Therefore, excluding Gaul a priori from silver provenance studies may introduce significant bias.

As a closing remark, silver production by a particular mining district is difficult to evaluate, first because reliable numbers are missing and, second, because some mining works may not have been preserved. In addition, many potentially important samples have become notoriously difficult to obtain. Thanks to the proximity of active silver mines, mints of Athens and Thasos in Greek times stroke local production (Albarede et al., 2024a). In contrast, the Lugdunum (Lyon) workshops from the Late Roman Republic and Early Empire are located far from any significant source of bullion, but are nevertheless known to have processed large silver issues (Sutherland, 1984). Production estimates may also be amplified for political reasons at the time, notably as communication warfare. Moreover, mints concentrated artisanal expertise, skillful engravers, and well-trained slaves, and as such may have attracted non-domestic bullion.

Conclusions

New Ag and Pb isotope compositions on galena samples from southern Sardinia suggest that silver extracted from local mines is different from the most common bullion used to mint silver coinage. The connection between *hacksilver* hoards from the Levant and ores from Sardinia is confirmed. At this stage, however, the overall number of samples analyzed is still too small to assess whether Sardinian ores were a major contributor to Greek and Roman silver bullion.

² κατὰ γοῦν τὴν Γαλατίαν ἄργυρος μὲν οὐ γίνεται τὸ σύνολον (Throughout Gaul there is found practically no silver).

Mines from southern Gaul produced silver with a range of Ag isotope compositions that render these ores consistent with those of the main silver pool (group 1). Hence, not including this area among the significant silver sources in antiquity reflects biases of ancient literature, which does not mention southern Gaul, and on the lack of archeological evidence for major mining works. As far as Pb and Ag isotopes are concerned, southern Gaul cannot be excluded as a potential source of silver bullion.

Acknowledgements. We thank Eloise Gaillou from the Mineralogy Museum of Mines ParisTech for access to samples from southern France and to some from Sardinia, and Guillaume Estrade for guiding us through the publications on ores from southern France. Insightful comments from four anonymous reviewers allowed significant improvements to the text.

Funding declaration. This work was funded by the Advanced Grant 741454-SILVER-ERC-2016-ADG 'Silver Isotopes and the Rise of Money' awarded to FA by the European Research Council.

Competing interests. The authors declare no competing interests as defined by Springer, or other interests that might be perceived to influence the results and/or discussion reported in this paper.

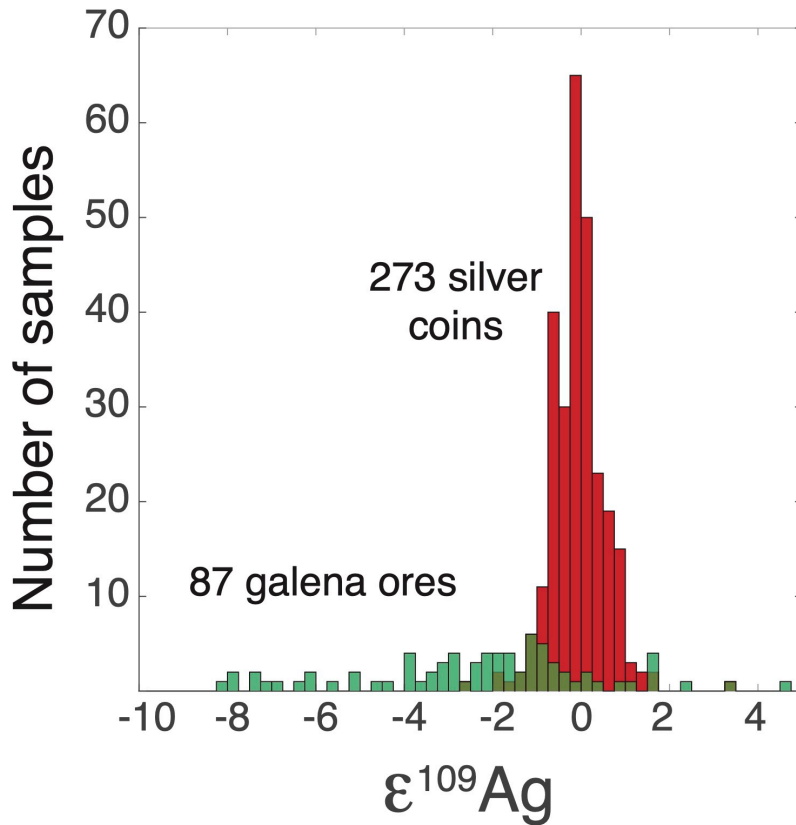


Figure 1. Histogram of Ag isotope compositions of coins from ancient Greece, Persia, Rome (Albarède et al., 2016, Desaulty et al., 2011, Milot et al., 2021b, Vaxevanopoulos et al., 2022), medieval Europe (Desaulty et al., 2011), Tudor England (Desaulty and Albarede, 2013), and Spanish colonial Americas (Desaulty et al., 2011). The $\epsilon_{109\text{Ag}}$ value of all but five of the 273 silver coins plot in the interval -1 to $+1$ (-0.1 to $+0.1$ permil). The spread of $\epsilon_{109\text{Ag}}$ values in ores is much broader than in coins. Ores with $\epsilon_{109\text{Ag}}$ values outside of the coin range can be excluded as sources of the silver used for minting.

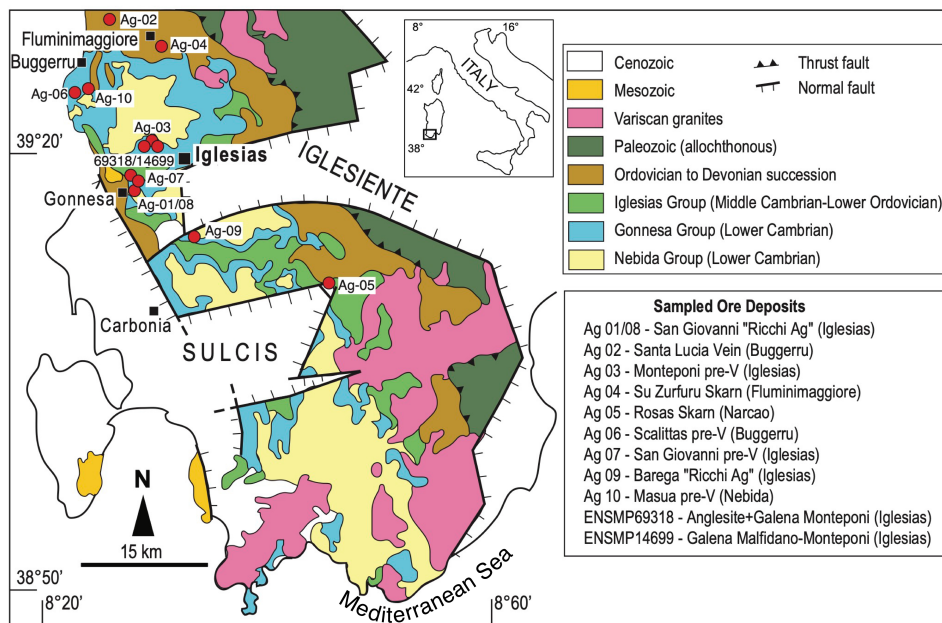


Figure 2. Geological map of southwestern Sardinia with the locations of the samples analyzed in the present work (red circles) (Boni, unpublished work).

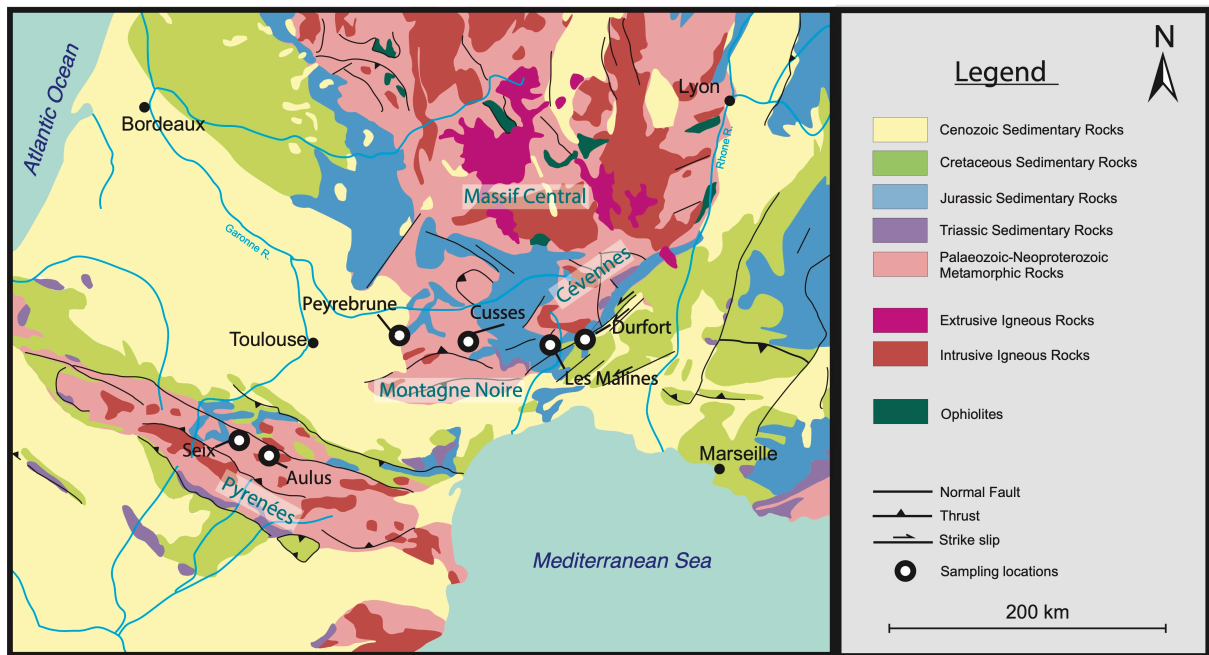


Figure 3. Simplified geological map of southern France with the locations of the samples analyzed in the present work (modified after Asch (2005)).

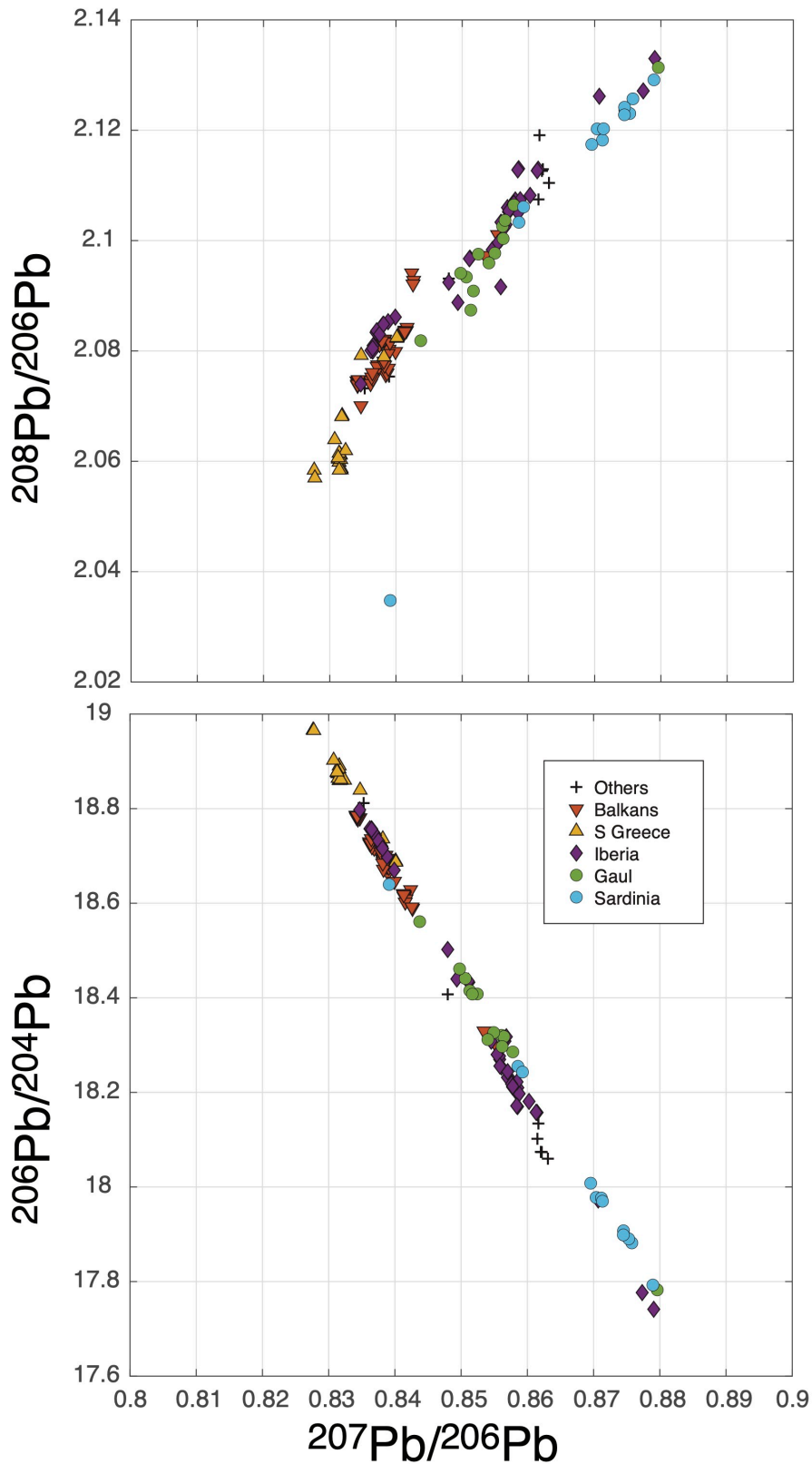


Figure 4. Conventional Pb isotope plots for Sardinia and southern France. Iberian samples and ‘others’ from Milot et al. (2021b, 2022). Southern Greece and the Balkans, including Laurion, Macedonia, and Thrace from Vaxevanopoulos et al. (2022). Balkans (incl. Thrace and Macedonia) from Westner et al. (2023). ‘Others’ stand for localities that do not belong to these regions.

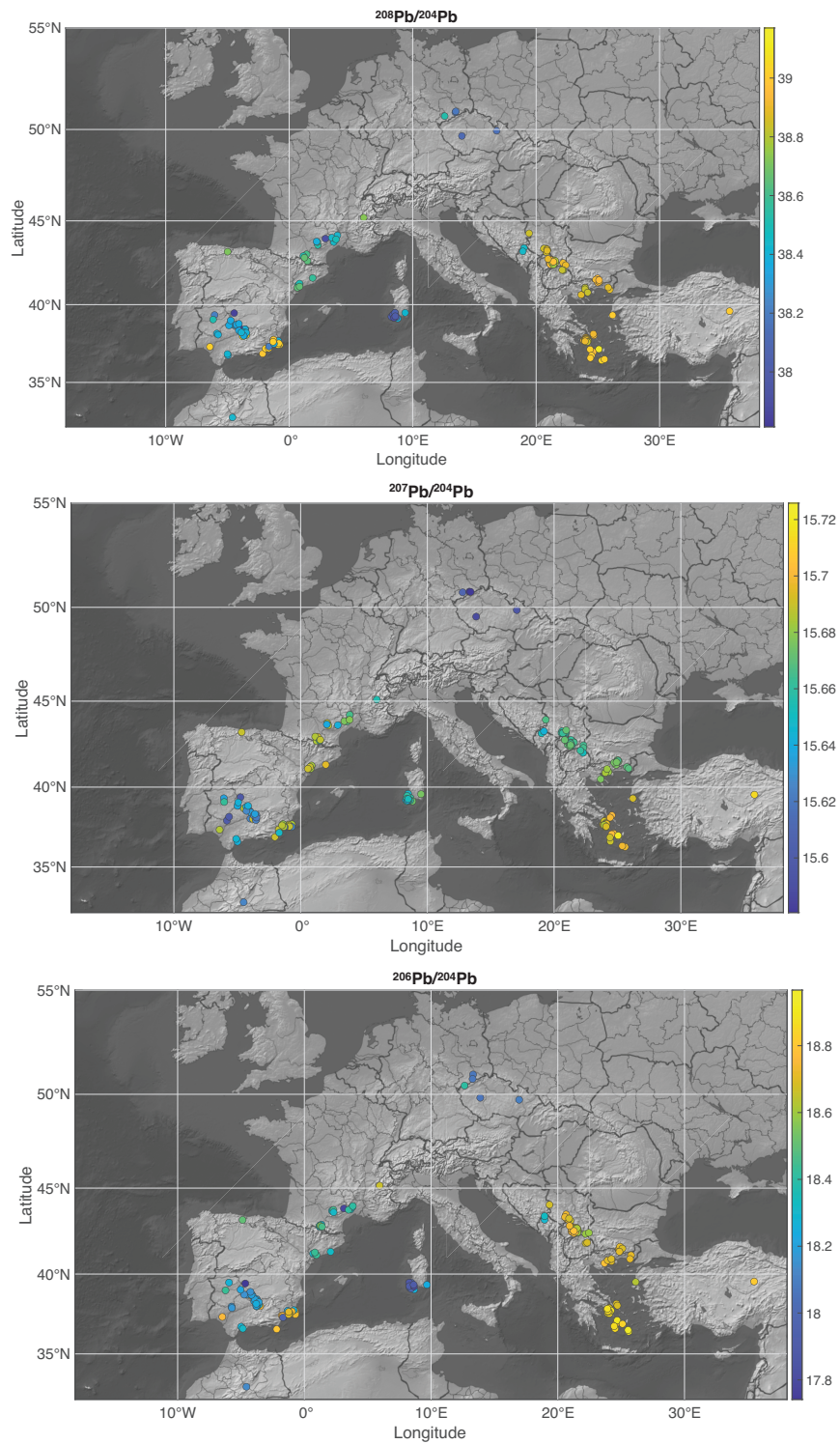


Figure 5. Map of the ^{204}Pb -normalized ratios for samples for which Ag isotopes are also known (from this work and the literature (Milot et al., 2021b, Milot et al., 2022, Vaxevanopoulos et al., 2022, Westner et al., 2023)). Note the strong clustering of some silver ore provinces.

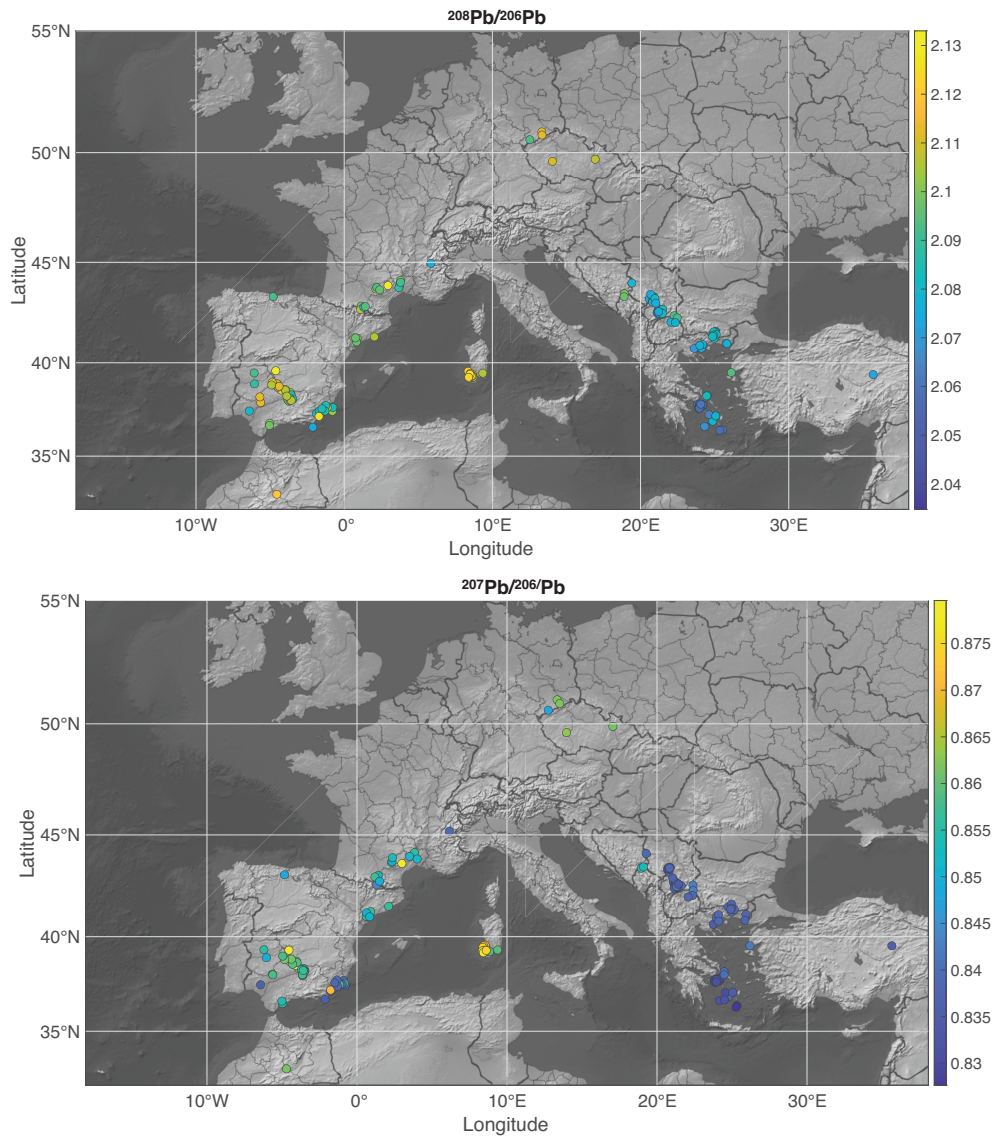


Figure 6. Map of the ^{206}Pb -normalized ratios for samples for which Ag isotopes are also known.

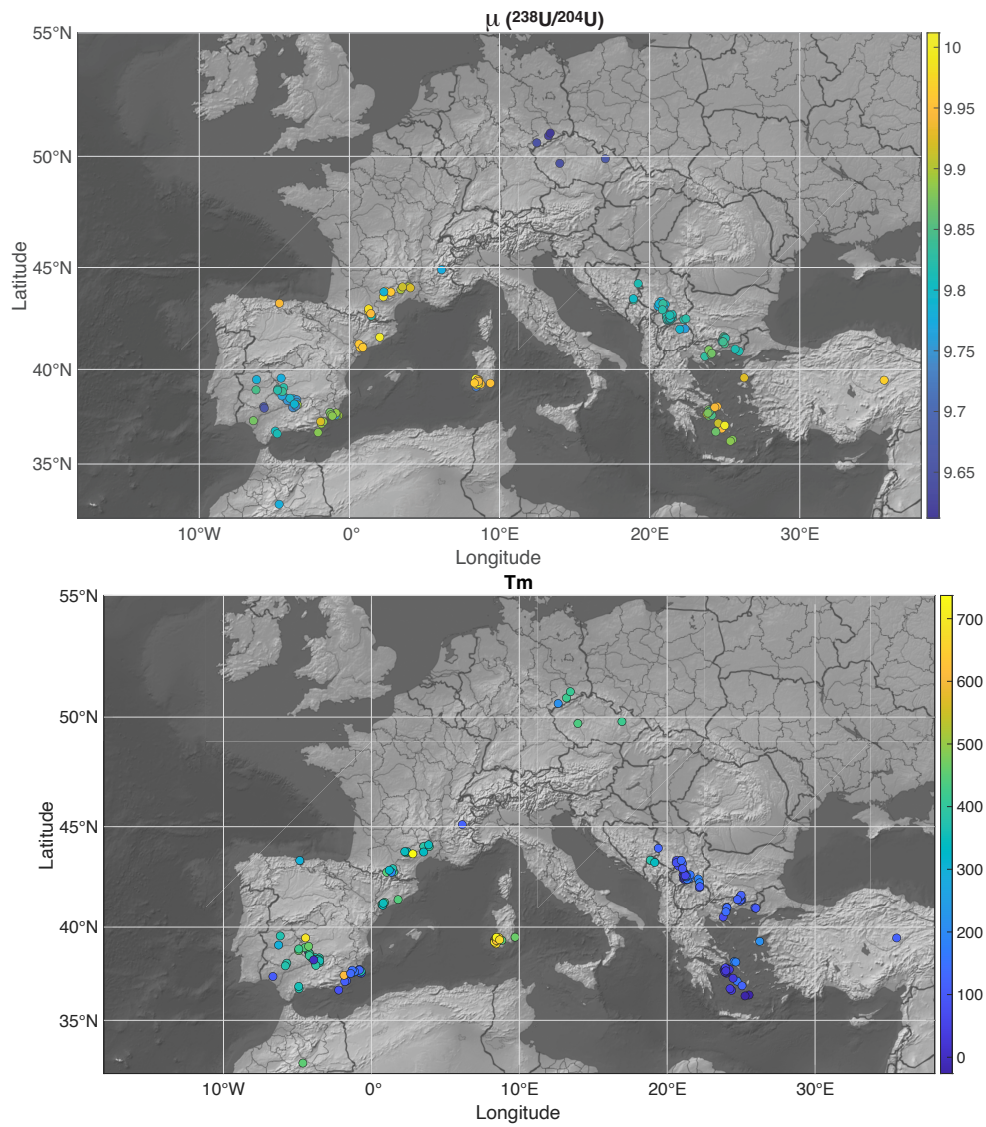


Figure 7. Map of the Pb model age T_m , μ ($^{238}\text{U}/^{204}\text{Pb}$), and κ ($^{232}\text{Th}/^{238}\text{U}$) values for samples for which Ag isotopes are also known.

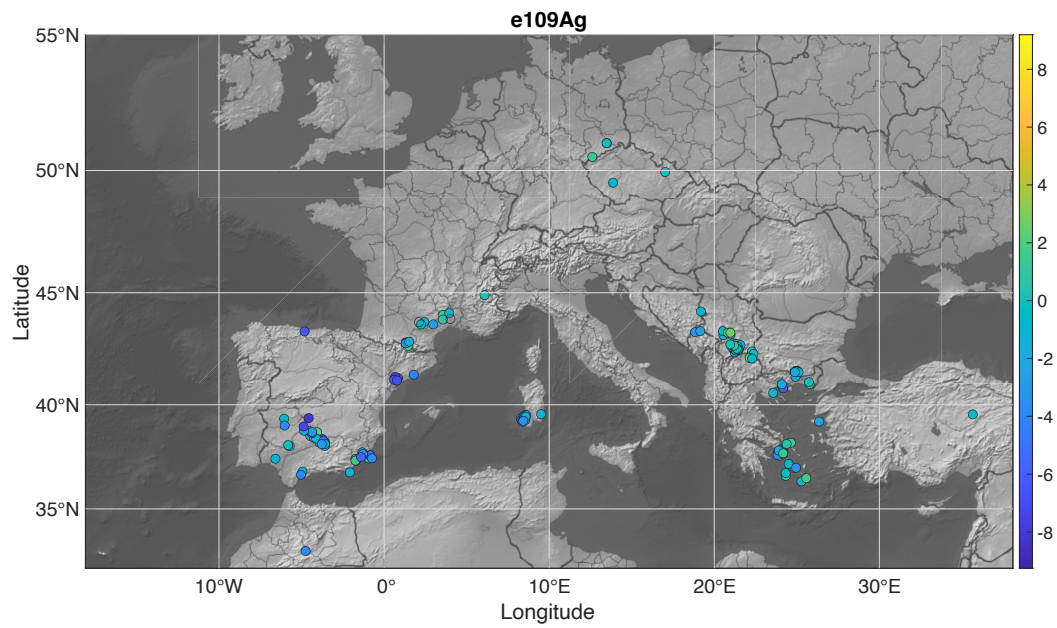


Figure 8. Map of the $\epsilon_{109\text{Ag}}$ values of the galena samples analyzed in this work (Sardinia and southern France) together with literature values.

References

- Abraham P (2000) Les mines d'argent antiques et médiévales du district minier de Kaymar (nord-ouest de l'Aveyron), Gallia - Archéologie de la France antique. Mines et métallurgies en Gaule. 57, 123-127
- Albarede F, Davis G, Blichert-Toft J, Gentelli L, Gitler H, Pinto M, Telouk P (2024a) A new algorithm for using Pb isotopes to determine the provenance of bullion in ancient Greek coinage, Journal of Archaeological Science 163, 105919
- Albarede F, Davis G, Gentelli L, Blichert-Toft J, Gitler H, Pinto M, Telouk P (2024b) Bullion mixtures in silver coinage from ancient Greece and Egypt, Journal of Archaeological Science 162, 105918
- Albarède F, Desaulty AM, Blichert-Toft J (2012) A geological perspective on the use of Pb isotopes in archaeometry, Archaeometry 54, 853-867
- Albarède F, Blichert-Toft J, Rivoal M, Telouk P (2016) A glimpse into the Roman finances of the Second Punic War through silver isotopes, Geochemical Perspective Letters 2, 127-137
- Albarède F, Blichert-Toft J, Gentelli L, Milot J, Vaxevanopoulos M, Klein S, Westner K, Birch T, Davis G, de Callatay F (2020) A miner's perspective on Pb isotope provenances in the Western and Central Mediterranean, Journal of Archaeological Science 121, 105194
- Álvaro JJ, Bauluz B, Imaz AG, Simón JL (2008) Multidisciplinary constraints on the Cadomian compression and early Cambrian extension in the Iberian Chains, NE Spain, Tectonophysics 461, 215-227
- Arribas A, Mathur R, Megaw P, Arribas I (2020) The isotopic composition of Ag in ore minerals, Geochemistry Geophysics Geosystems 21, e2020GC009097
- Asch K (2005). IGME 5000: 1 : 5 Million International Geological Map of Europe and Adjacent Areas, Bundesanstalt für Geowissenschaften und Rohstoffe, Hannover
- Baron S, Carignan J, Laurent S, Ploquin A (2006) Medieval lead making on Mont-Lozère Massif (Cévennes-France): tracing ore sources using Pb isotopes, Applied geochemistry 21, 241-252
- Bechstädt T, Boni M (1994). Sedimentological, stratigraphical and ore deposits field guide of the autochthonous Cambro-Ordovician of Southwestern Sardinia, Istituto poligrafico e zecca dello stato
- Berger D, Brauns M, Brüggmann G, Pernicka E, Lockhoff N (2021) Revealing ancient gold parting with silver and copper isotopes: implications from cementation experiments and for the analysis of gold artefacts, Archaeological and Anthropological Sciences 13, 1-27
- Boni M, Koeppl V (1985) Ore-lead isotope pattern from the Iglesiente-Sulcis Area (SW Sardinia) and the problem of remobilization of metals, Mineral. Deposita 20, 185-193
- Boni M, Balassone G, Iannace A (1996) Base metal ores in the Lower Paleozoic of southwestern Sardinia,
- Bonsangue ML (2011). Administrer et exploiter les mines en Gaule méridionale: le rôle de Narbonne (ier siècle av. J.-C.-iiie siècle ap. J.-C.), in: Benoist, S., Daguet-Gagey, A., Hoët-Van Cauwenberghe, C. (Eds.), Figures d'empire, fragments de mémoire:

- pouvoirs et identités dans le monde romain impérial (IIe s. av. n. è.-IIIe s. ap. n. è.), Presses Universitaires du Septentrion, Villeneuve-d'Ascq, pp. 361-384
- Brevart O, Dupre B, Allegre CJ (1982) Metallogenic provinces and the remobilization process studied by lead isotopes; lead-zinc ore deposits from the southern Massif Central, France, *Economic Geology* 77, 564-575
- Casas J (2010) Ordovician deformations in the Pyrenees: new insights into the significance of pre-Variscan ('sardic') tectonics, *Geological Magazine* 147, 674-689
- Casas JM, Álvaro J, Clausen S, Padel M, Puddu C, Sanz-López J, Sánchez-García T, Navidad M, Castiñeiras P, Liesa M (2019). Palaeozoic basement of the Pyrenees, *The Geology of Iberia: A Geodynamic Approach: Volume 2: The Variscan Cycle*, Springer, pp. 229-259
- Charef A (1986) La nature et le rôle des phases associées à la minéralisation Pb-Zn dans les formations carbonatées et leurs conséquences métallogéniques. Etude des inclusions fluides et des isotopes (H, C, O, S, Pb) des gisements des Malines (France), Fedj-el-Adoum et Jbel Hallouf-Sidi Bou Aouane (Tunisie), Thèse d'état, Nancy
- Cherchi A, Montadert L (1982) Oligo-Miocène rift of Sardinia and the early history of the western Mediterranean basin, *Nature* 298, 736-739
- Craddock PT (1995). Early metal mining and production, Edinburgh University Press
Edinburgh
- Cugeron A, Oliot E, Chauvet A, Gavaldà Bordes J, Laurent A, Le Goff E, Cenki-Tok B (2018) Structural control on the formation of Pb-Zn deposits: An example from the Pyrenean Axial Zone, *Minerals* 8, 489
- De Caro T, Riccucci C, Parisi EI, Faraldi F, Caschera D (2013) Ancient silver extraction in the Montevecchio mine basin (Sardinia, Italy): micro-chemical study of pyrometallurgical materials, *Applied Physics A* 113, 945-957
- de Madinabeitia SG, Ibarra JG, Zalduendo JS (2021) IBERLID: A lead isotope database and tool for metal provenance and ore deposits research, *Ore Geology Reviews* 137, 104279
- Denèle Y, Laumonier B, Paquette J-L, Olivier P, Gleizes G, Barbey P (2014) Timing of granite emplacement, crustal flow and gneiss dome formation in the Variscan segment of the Pyrenees, *Geological Society, London, Special Publications* 405, 265-287
- Desaulty AM, Telouk P, Albalat E, Albaredo F (2011) Isotopic Ag-Cu-Pb record of silver circulation through 16th-18th century Spain, *Proceedings of the National Academy of Sciences of the United States of America* 108, 9002-9007
- Desaulty AM, Albaredo F (2013) Copper, lead, and silver isotopes solve a major economic conundrum of Tudor and early Stuart Europe, *Geology* 41, 135-138
- Domergue C, Leroy M (2000) L'état de la recherche sur les mines et les métallurgies en Gaule, de l'époque gauloise au haut Moyen Âge, *Gallia* 57, 3-10
- Domergue C, Rico C (2003) Questions sur l'origine des lingots de métal trouvés au large des côtes du Languedoc et du Roussillon, *Revue archéologique de Narbonnaise. Suppléments*, 389-399
- Domergue C, Serneels V, Cauuet B, Paillet J-M, Orzechowski S (2006) Mines et métallurgies en Gaule à la fin de l'âge du Fer et à l'époque romaine, *Celtes et Gaulois, l'Archéologie face à l'histoire* 5, 131-162
- Dubois C (1997) Les anciennes mines de plomb argentifère de l'Ariège, Pallas: Mélanges Claude Domergue 46, 233-238

- Eshel T, Yahalom-Mack N, Shalev S, Tirosh O, Erel Y, Gilboa A (2018) Four iron age silver hoards from Southern Phoenicia: From bundles to Hacksilber, *Bulletin of the American Schools of Oriental Research* 379, 197-228
- Eshel T, Erel Y, Yahalom-Mack N, Tirosh O, Gilboa A (2019) Lead isotopes in silver reveal earliest Phoenician quest for metals in the west Mediterranean, *Proceedings of the National Academy of Sciences* 116, 6007-6012
- Eshel T, Gilboa A, Yahalom-Mack N, Tirosh O, Erel Y (2021) Debasement of silver throughout the Late Bronze–Iron Age transition in the Southern Levant: Analytical and cultural implications, *Journal of Archaeological Science* 125, 105268
- Eshel T, Erel Y, Yahalom-Mack N, Tirosh O, Gilboa A (2022) From Iberia to Laurion: Interpreting Changes in Silver Supply to the Levant in the Late Iron Age Based on Lead Isotope Analysis, *Archaeological and Anthropological Sciences* 14, 120
- Feugère M, Py M (2007). Emissions et circulation monétaires chez les Rutènes avant Auguste.. *Colloque de Rodez et Millau (Aveyron), Rodez et Millau*, pp. 297-312
- Franceschelli M, Puxeddu M, Cruciani G (2005) Variscan metamorphism in Sardinia, Italy: review and discussion, *Journal of the Virtual Explorer* 19, 2-36
- Fujii T, Albarede F (2018) ^{109}Ag – ^{107}Ag fractionation in fluids with applications to ore deposits, archeometry, and cosmochemistry, *Geochimica et Cosmochimica Acta* 234, 37-49
- Gentelli L, Blichert-Toft J, Davis G, Gitler G, Gitler H, Albarede F (2021) Metal provenance of Late Bronze to Iron Age Hacksilber hoards in the southern Levant, *Journal of Archaeological Sciences* 134, 105472
- Guérangé-Lozes J, Guérangé B, Lefavrais A, Rançon J, Astruc J, Michard A, Greber C, Servelle C (1982). Notice explicative de la feuille de Camarès à 1/50 000, BRGM, Orléans
- Guitard G, Vielzeuf D, Martinez F (1995). Le Métamorphisme Hercynien, in: Barnolas, A., Chiron, J.C. (Eds.), *Synthèse Géologique et Géophysique des Pyrénées - Vol. 1* Editions BRGM - ITGE, Orléans, pp. 501-584
- Hirt A (2020). Gold and Silver Mining in the Roman Empire, in: Butcher, K. (Ed.), *Debasement. Manipulation of Coin Standards in Pre-Modern Monetary Systems*, Oxbow books, Oxford Philadelphia, pp. 111-124
- Ingo G, Agus T, Ruggeri R, Bonapasta AA, Bultrini G, Chiozzini G (1996) Lead and Silver Production in the Montevecchio Basin (Western Sardinia, Italy), *MRS Online Proceedings Library (OPL)* 462
- Jolivet L, Faccenna C (2000) Mediterranean extension and the Africa-Eurasia collision, *Tectonics* 19, 1095-1106
- Klein S, Rose T, Westner KJ, Hsu YK (2022) From OXALID to GlobalID: Introducing a modern and FAIR lead isotope database with an interactive application, *Archaeometry* 64, 935-950
- Laumonier B, Canérot J, Colin J, Platel J, Bilotte M (2008). Les Pyrénées pré-hercyniennes et hercyniennes, in: l'Adour, U.d.P.e.d.p.d. (Ed.), *Pyrénées d'hier et d'aujourd'hui*, Atlantica, Pau, pp. 23-35
- Le Guen M, Orgeval J-J, Lancelot J (1991) Lead isotope behaviour in a polyphased Pb-Zn ore deposit: Les Malines (Cévennes, France), *Mineralium Deposita* 26, 180-188
- Le Guen M, Lescuyer J, Marcoux E (1992) Lead-isotope evidence for a Hercynian origin of the Salsigne gold deposit (Southern Massif Central, France), *Mineralium Deposita* 27, 129-136
- Lescuyer J-L, Giot D (1987). Les minéralisations Pb, Zn de Montagne Noire et leurs relations avec leur encaissant cambrien carbonaté: sur quelques exemples du versant Nord, La

- Rabasse, Brusque, Lardenas, Peux, Les Comtes et du versant Sud, Bibaud, Tête Rousse., Contrôle des minéralisations Pb, Zn, Cu, Ag, Au de la Province cambrienne, Bureau de recherches géologiques et minières, Orleans
- Leveque M-H (1990). Contribution of U-Pb geochronology to characterizing the Cadomian magmatism of the southeastern French Massif Central and of the related uranium-ore at Bertholene, Faculte des Sciences, Montpellier, p. 347
- Marcoux E, Moelo Y (1991) Lead isotope geochemistry and paragenetic study of inheritance phenomena in metallogenesis; examples from base metal sulfide deposits in France, *Economic Geology* 86, 106-120
- Marcoux É (1987). Isotopes du plomb et paragenèses métalliques, traceurs de l'histoire des gîtes minéraux: illustration des concepts de source, d'héritage et de régionalisme dans les gîtes français applications en recherche minière, Université de Clermont II, Editions du Bureau de Recherches Géologiques et Minières, Clermont-Ferrand
- Marignac C, Cuney M (1999) Ore deposits of the French Massif Central: insight into the metallogenesis of the Variscan collision belt, *Mineralium Deposita* 34, 472-504
- Milot J, Blichert-Toft J, Sanz MA, Fetter N, Télouk P, Albarède F (2021a) The significance of galena Pb model ages and the formation of large Pb-Zn sedimentary deposits, *Chemical Geology* 583, 120444
- Milot J, Malod-Dognin C, Blichert-Toft J, Télouk P, Albarède F (2021b) Sampling and combined Pb and Ag isotopic analysis of ancient silver coins and ores, *Chemical Geology* 564, 120028
- Milot J, Blichert-Toft J, Sanz MA, Malod-Dognin C (2022) Silver isotope and volatile trace element systematics in galena samples from the Iberian Peninsula and the quest for silver sources of Roman coinage, *Geology* 50
- Munoz M (1997) Le filon (Zn, F) de Peyrebrune (SW Massif central, France): caractérisation géochimique des fluides au cours du Mésozoïque à la bordure orientale du bassin d'Aquitaine, *Comptes Rendus de l'Académie des Sciences-Series IIA-Earth and Planetary Science* 324, 899-906
- Munoz M, Baron S, Boucher A, Beziat D, Salvi S (2016) Mesozoic vein-type Pb–Zn mineralization in the Pyrenees: Lead isotopic and fluid inclusion evidence from the Les Argentières and Lacore deposits, *Comptes Rendus Geoscience* 348, 322-332
- Orgeval J, Caron C, Lancelot J, Omenetto P, Gandin A, Libertà A, Courjault Radé P, Tollon F, Laurent P, Maluski H (2000) Genesis of polymetallic and precious-metal ores in the Western Mediterranean province (Cévennes, France–Sardinia, Italy), *Applied Earth Science* 109, 77-94
- Orlandi P, Gelosa M (2007) Argentiera della Nurra. I minerali di alterazione della miniera di sfalerite e galena argentifera., *Rivista Mineralogica Italiana* 31, 22-31
- Pearce M (2017) The 'island of silver veins': an overview of the earliest metal and metalworking in Sardinia, *Metalla* 23, 91-111
- Ploquin A, Allée P, Bailly-Maître M-C, Baron S, De Beaulieu J-L, Carignan J, Laurent S, Lavoie M, Le Carlier CM, Paradis S (2010) PCR–Le plomb argentifère ancien du Mont Lozère (Lozère). A la recherche des mines, des minerais et des ateliers, des paysages et des hommes, *ArcheoSciences. Revue d'archéométrie*, 99-114
- Puddu C, Casa Tuset JM, Blasco A, Javier J (2021). The Sardinic Phase in the Ordovician of Southern Sardinia and Eastern Pyrenees: Stratigraphic, Structural and Magmatic Constraints, *Universidad de Zaragoza*

- Rehault J-P, Boillot G, Mauffret A (1984) The western Mediterranean basin geological evolution, *Marine Geology* 55, 447-477
- Romagny A, Jolivet L, Menant A, Bessièrè E, Maillard A, Canva A, Gorini C, Augier R (2020) Detailed tectonic reconstructions of the Western Mediterranean region for the last 35 Ma, insights on driving mechanisms, *Bulletin de la Société géologique de France* 191, 37
- Santoro L, Boni M, Putzolu F, Mondillo N (2023). Base-metal sulphides and barite in the Palaeozoic of SW Sardinia: From tectonically deformed SedEx and Irish-type deposits to post-Variscan hydrothermal karst and vein ores, in: Andrew, C.J., Hitzman, M.W., Stanley, G. (Eds.), *Irish-Type Deposits around the World*, Irish Association for Economic Geology, Dublin, pp. 425-442
- Schettino A, Turco E (2011) Tectonic history of the western Tethys since the Late Triassic, *Geological Society of America Bulletin* 123, 89-105
- Stos-Gale ZA, Gale NH (2009) Metal provenancing using isotopes and the Oxford archaeological lead isotope database (OXALID), *Archaeological and Anthropological Sciences* 1, 195-213
- Stos-Gale ZA, Davis G (2020). The minting/mining Nexus: New understandings of Archaic Greek silver coinage from lead isotope analysis, in: Sheedy, K., Davis, G. (Eds.), *Metallurgy in Numismatics 6: : Mines, Metals and Money: Ancient World Studies in Science, Archaeology and History*, Royal Numismatic Society, London, pp. 87-100
- Sutherland CHV (1984). *Roman Imperial Coinage. Volume I*, Spink Books, London
- Terpstra TT (2021) Mediterranean silver production and the site of Antas, Sardinia, *Oxford Journal of Archaeology* 40, 176-190
- Tisseyre P, Tusa S, Cairns WR, Bottacin FS, Barbante C, Ciriminna R, Pagliaro M (2008) The lead ingots of Capo Passero: Roman global Mediterranean trade, *Oxford Journal of Archaeology* 27, 315-323
- Trincherini PR, Barbero P, Quarati P, Domergue C, Long L (2001) Where Do the Lead Ingots of the Saintes-maries-de-la-mer Wreck Come From? *Archaeology Compared With Physics, Archaeometry* 43, 393-406
- Trincherini PR, Domergue C, Manteca I, Nesta A, Quarati P (2009) The identification of lead ingots from the Roman mines of Cartagena: the role of lead isotope analysis, *Journal of Roman Archaeology* 22, 123-145
- Valera RG, Valera P, Rivoldini A (2005a) Sardinian ore deposits and metals in the Bronze Age, *Monographies Instrumentum* 90, 43-87
- Valera RG, Valera P, Rivoldini A (2005b). The Sardinian mineral deposits in the Bronze Age, in: Schiavo, F.L., Giumlia-Mair, A., Valera, R., Sanna, U. (Eds.), *Archaeometallurgy in Sardinia*, Monique Mergoïl, Montagnac, pp. 43-87
- Vaxevanopoulos M, Davis G, Milot J, Blichert-Toft J, Malod-Dognin C, Albarède F (2022) Narrowing provenance for ancient Greek silver coins using Ag isotopes and Sb contents of potential ores, *Journal of Archaeological Science* 145, 105645
- Wagner GA, Pernicka E, Seeliger TC, Öztunali Ö, Baranyi I, Begemann F, Schmitt-Strecker S (1985) Geologische Untersuchungen zur frühen Metallurgie in NW-Anatolien,, *Bulletin of the Mineral Research and Exploration Institute of Turkey* 101, 45–81
- Wang J-L, Wei H-Z, Williams-Jones A, Dong G, Zhu Y-F, Jiang S-Y, Ma J, Hohl SV, Liu X, Li Y-C (2022) Silver isotope fractionation in ore-forming hydrothermal systems, *Geochimica et Cosmochimica Acta* 322, 24-42

- Westner KJ, Vaxevanopoulos M, Blichert-Toft J, Davis G, Albarède F (2023) Isotope and trace element compositions of silver-bearing ores in the Balkans as possible metal sources in antiquity, *Journal of Archaeological Science* 155, 105791
- Yigit O (2009) Mineral deposits of Turkey in relation to Tethyan metallogeny: implications for future mineral exploration, *Economic Geology* 104, 19-51
- Yigit O (2012) A prospective sector in the Tethyan Metallogenic Belt: Geology and geochronology of mineral deposits in the Biga Peninsula, NW Turkey, *Ore Geology Reviews* 46, 118-148

Table 1. Ore localities, Pb and Ag isotope data, and trace-element data of the samples analyzed

Lab code	Locality	Province	Mineralogy	Geological age
<i>Sardinia</i>				
Ag-01	San Giovanni Mine	Iglesias	Ricchi Ag	post-Variscan
Ag-02	Santa Lucia	Buggerru	Fluorite-Barite-C	post-Variscan
Ag-03	Monteponi Mine	Iglesias	Masse Centrali	pre-Variscan
Ag-04	Su Zurfuru	Fluminimaggiore	Fluorite-Galena	pre- to syn-Variscan
Ag-05	Rosas Mine	Narcao	skarn	syn-Variscan
Ag-06	Scalittas Mine	Buggerru		pre-Variscan
Ag-07	San Giovanni Mine	Iglesias	Cantiere Contati	pre-Variscan
Ag-08	San Giovanni Mine	Iglesias	Ricchi Ag	post-Variscan
Ag-09	Barega Mine	Iglesias	Ricchi Ag	post-Variscan
Ag-10	Masua Mine	Masua		pre-Variscan
ENSMP69318	Monteponi	Iglesias	anglesite, galena	
ENSMP57149	Sarrabus	Cagliari	acanthite (argyrite), galena	
ENSMP14699	Malfidano	Buggerru	galena	
<i>Southern France</i>				
65644	L'Argentière shaft, Aulus, Ariège		galena	Paleozoic
65726	Lauqueille, Aulus, Ariège		galena	Paleozoic
65649	Aulus- les- Bains, Ariège		galena	Paleozoic
27826	Les Abères, Vallée de Rivernère, Ariège		galena	Paleozoic
65647	Seix, Ariège / Dietrich Collection		galena	Paleozoic
59051	Peyrebrune, Tarn		galena	Paleozoic
Galene Tarn	Peyrebrune, Tarn		galena	Paleozoic
59040	Peyrebrune, Tarn		galena	Paleozoic
63600	Cusses Brusque, Aveyron		bournonite	Paleozoic
S-38	Les Malines, St Laurent du Gard		cerusite	Paleozoic
63025	Les Malines, St Laurent du Gard		galena	Paleozoic
27854	St-Félix- de- Pallières, Gard		galena	Paleozoic
Galène Durfort	Galène mine de Durfort, Gard		galena	Paleozoic
Lab code	$^{206}\text{Pb}/^{204}\text{Pb}$	2 sigma	$^{207}\text{Pb}/^{204}\text{Pb}$	2 sigma
<i>Sardinia</i>				
Ag-01	18.6396	0.0017	15.6412	0.0013
Ag-02	17.9778	0.0006	15.6475	0.0005
Ag-03	17.8984	0.0006	15.6530	0.0006
Ag-04	17.9765	0.0005	15.6607	0.0004
Ag-05	18.2551	0.0004	15.6732	0.0004
Ag-06	17.8817	0.0010	15.6604	0.0007
Ag-07	17.8903	0.0011	15.6594	0.0009
Ag-08	18.0079	0.0004	15.6590	0.0003

Ag-09	17.9699	0.0005	15.6579	0.0005
Ag-10	17.9074	0.0006	15.6603	0.0004
ENSMP69318	17.7926	0.0008	15.6389	0.0007
ENSMP57149	18.2430	0.0006	15.6756	0.0005
ENSMP14699	17.8986	0.0006	15.6522	0.0006
<i>Southern France</i>				
65644	18.3207	0.0006	15.6846	0.0006
65726	18.5610	0.0012	15.6608	0.0009
65649	18.4612	0.0011	15.6878	0.0009
27826	18.4081	0.0006	15.6918	0.0006
65647	18.2856	0.0007	15.6854	0.0006
59051	18.3178	0.0016	15.6885	0.0014
Galene Tarn	18.3117	0.0015	15.6388	0.0012
59040	18.4409	0.0005	15.6865	0.0004
63600	17.7824	0.0009	15.6419	0.0009
S-38	18.4151	0.0008	15.6767	0.0007
63025	18.3266	0.0005	15.6681	0.0004
27854	18.2968	0.0007	15.6656	0.0006
Galène Durfort	18.4078	0.0012	15.6782	0.0009
	#N/A			

Lab code	Ca ppm	Mn ppm	Fe ppm	Ni ppm
<i>Sardinia</i>				
Ag-01	207	2	520	47
Ag-02	752	16	126	198
Ag-03	419	171	6846	185
Ag-04	4553	21	462	148
Ag-05	3891	798	3891	18
Ag-06	541	6	39	349
Ag-07	310	8	91	41
Ag-08	321	1	258	86
Ag-09	1010	30	501	87
Ag-10	477	12	406	225
ENSMP69318	313	13	976	-6
ENSMP57149	3264	302	182	113
ENSMP14699	533	52	374	122
<i>Southern France</i>				
65644	243	3	2696	42
65726	-8	4564	38589	141
65649	5676	110	1826	92
27826	-166	112	8867	150
65647	6758	731	7125	214
59051	180	6	304	18.2

Galene Tarn	–	96	1236	98
59040	12989	5738	78196	147
63600	356	63	4626	73
S-38	372	21	1001	52
63025	5832	541	10327	42
27854	418	63	2396	46
Galène Durfort	3228	21	548	10

'–' stands for below detection.

latitude N longitude E ore typology

39.280	8.475	post-Variscan low-temperature veins and paleokarst fillings
39.442	8.465	skarn and high-temperature veins
39.304	8.508	stratabound ores in Cambrian carbonates
39.430	8.503	skarn and high-temperature veins
39.203	8.720	skarn and high-temperature veins
39.373	8.424	skarn and high-temperature veins
39.289	8.484	skarn and high-temperature veins
39.281	8.477	post-Variscan low-temperature veins and paleokarst fillings
39.255	8.534	post-Variscan low-temperature veins and paleokarst fillings
39.364	8.439	stratabound ores in Cambrian carbonates
39.304	8.508	stratabound ores in Cambrian carbonates
39.419	9.542	skarn and high-temperature veins
39.304	8.508	stratabound ores in Cambrian carbonates
42.778	1.392	sedimentary-exhalative Pb–Zn deposits
42.780	1.375	sedimentary-exhalative Pb–Zn deposits
42.781	1.373	sedimentary-exhalative Pb–Zn deposits
42.953	1.268	sedimentary-exhalative Pb–Zn deposits
42.867	1.178	sedimentary-exhalative Pb–Zn deposits
43.762	2.251	vein type
43.762	2.251	vein type
43.762	2.251	vein type
43.792	2.944	strata-bound Pb-Zn ores are found in Cambrian carbonates
43.920	3.618	strata-bound Pb-Zn ores are found in Cambrian carbonates
43.921	3.618	strata-bound Pb-Zn ores are found in Cambrian carbonates
44.045	3.939	strata-bound Pb-Zn ores are found in Cambrian carbonates
43.996	3.940	strata-bound Pb-Zn ores are found in Cambrian carbonates

$^{208}\text{Pb}/^{204}\text{Pb}$	2 sigma	$^{207}\text{Pb}/^{206}\text{Pb}$	2 sigma	$^{208}\text{Pb}/^{206}\text{Pb}$	2 sigma	$\epsilon_{109}\text{Ag}$
37.927	0.002	0.83911	0.00001	2.03467	0.00009	-1.40
38.117	0.001	0.87038	0.00001	2.12024	0.00004	-9.25
38.010	0.002	0.87455	0.00001	2.12359	0.00010	-4.38
38.078	0.002	0.87118	0.00001	2.11822	0.00011	-1.45
38.396	0.001	0.85857	0.00001	2.10332	0.00002	-4.12
38.011	0.001	0.87581	0.00001	2.12575	0.00007	-3.81
37.982	0.001	0.87531	0.00001	2.12299	0.00008	-4.02
38.131	0.001	0.86955	0.00001	2.11739	0.00006	-4.10

38.101	0.001	0.87134	0.00001	2.12028	0.00002	-4.66
38.038	0.001	0.87451	0.00000	2.12417	0.00002	-1.13
37.883	0.002	0.87895	0.00001	2.12906	0.00005	-1.36
38.421	0.001	0.85927	0.00001	2.10608	0.00006	-1.36
37.995	0.003	0.87449	0.00001	2.12276	0.00014	-3.35
38.521	0.001	0.85610	0.00001	2.10260	0.00003	1.48
38.642	0.002	0.84374	0.00001	2.08186	0.00002	-3.19
38.660	0.002	0.84977	0.00001	2.09409	0.00004	-1.60
38.612	0.002	0.85244	0.00001	2.09754	0.00003	-0.80
38.517	0.002	0.85781	0.00001	2.10645	0.00003	-4.12
38.535	0.003	0.85647	0.00001	2.10366	0.00006	-1.29
38.381	0.003	0.85403	0.00001	2.09594	0.00003	
38.605	0.001	0.85063	0.00001	2.09340	0.00002	-0.40
37.902	0.002	0.87961	0.00001	2.13138	0.00004	-2.60
38.438	0.004	0.85130	0.00001	2.08740	0.00019	0.98
38.444	0.001	0.85493	0.00001	2.09772	0.00005	1.43
38.430	0.002	0.85619	0.00001	2.10036	0.00003	-1.23
38.489	0.002	0.85170	0.00001	2.09087	0.00009	=NA()

Cu ppm	Zn ppm	Ag ppm	Cd ppm	Sn ppm	Sb ppm	Ba ppm
5444	168	200	43	2.6	291	1661
76	0	322	41	0.5	1184	47
70	7027	344	59	3.7	459	34
7	1098	955	79	10.4	624	2876
32	17042	487	251	3.3	367	8
30	168	103	13	0.4	107	3411
61	1098	200	54	1.8	12	9
558	482	630	10	177	2107	262
1023	325	709	20	2.8	1368	4412
58	2338	114	15	4.8	29	36851
129	10039	158	75	2.4	464	64
4	0	331679	3	2.6	175	44
9	45440	418	444	3.4	2	7
27	9666	2181	88	100	2247	7.3
699	231067	1490	673	10.0	1010	11711
1796	2838	1569	11	0.4	171	12
2	392	9	2	4.9	17	70
59	10387	193	42	4.6	336	8.2
8.8	36	290	8	14.3	435	3.1

3	11	368	7	8.7	697	-
112	1811	3282	7	1.9	4183	12
1636	1587	83	12	1.7	2337	1061
161	29202	524	139	1.0	620	62
361	121559	342	1307	1.9	5939	675
1126	204	637	11	3.6	1313	39
-	683	6	3	-0.2	337	1

Std error	T_m Ma	μ	κ
0.21	106	9.72	3.50
0.72	606	9.92	4.03
0.33	673	9.96	4.03
0.39	630	9.97	4.01
0.60	450	9.94	4.00
0.67	697	10.0	4.04
0.87	689	9.99	4.02
0.33	604	9.95	4.02

0.27	630	9.96	4.03
0.30	679	9.99	4.04
0.32	725	9.94	4.03
0.32	463	9.95	4.02
0.08	671	9.96	4.02
0.35	423	9.97	4.03
0.11	203	9.82	3.92
0.16	327	9.95	4.01
0.24	373	9.97	4.02
0.06	450	9.98	4.05
0.30	432	9.98	4.04
	346	9.79	3.94
0.45	340	9.95	3.99
0.18	737	9.96	4.05
0.08	340	9.91	3.92
0.15	389	9.90	3.98
0.42	406	9.90	3.99
	348	9.92	3.95

Pb ppm	Bi ppm
636462	10.4
702879	3.2
695225	1.7
601257	3.1
597468	245.5
682165	1.3
704245	1.3
551827	1.7
489128	0.8
577812	1.2
706689	1.0
268381	0.6
645453	1.2
794203	1.3
303968	0.8
737739	1.4
3315	0.1
648180	1.9
790327	1.2

1007995	2.1
389884	1.3
117410	3.2
745032	3.5
183360	0.4
760048	1.7
864715	2.1